Robust Light-Weight Magnetic-Based Door Event Detection with Smartphones

Liangyi Gong, Yiyang Zhao, Chaocan Xiang, Zhenhua Li, *Member, IEEE*, Chen Qian, *Member, IEEE*, and Panlong Yang, *Member, IEEE*

Abstract—Doors as densely-deployed natural landmarks play an important role in improving indoor positioning systems. However, the state-of-the-art door event detection works are based on either vision or infrastructure, thus incurring non-trivial device or management cost. To address these problems, we present a Light-weight Magnetic-based Door Event Detection method, called LMDD. It leverages built-in magnetic sensors of common smartphones to achieve infrastructure-free door event detection. After analyzing the special features of sensors' readings changes caused by the door, we design LMDD scheme with three main components, including data acquisition, events identification and events denoising. Moreover, an improved and robust door event detection framework based on a majority-voting model is proposed to fuse multiple-dimensional sensing data from non-magnetic built-in sensors. We have implemented a prototype of LMDD on Android-based platform. Experimental results show that LMDD with only magnetic sensor achieves door event detection accuracy of around 80 percent on average, ranging from 70 to 87 percent in various typical indoor environments. The enhanced LMDD based on the fusion of heterogeneous sensors can achieve a much higher door event detection accuracy of 90 percent on average.

Index Terms—Door event detection, magnetic-based, fusion of heterogeneous sensors, indoor positioning systems

1 Introduction

Indoor Positioning Systems (IPSes) have attracted wide attention, because it can effectively address the defects of GPS and localize the positions of devices in a building [25], [27], [40]. As illustrated in Fig. 1a, since the localization accuracy of current IPSes is limited by measurement and accumulation errors, they leverage various indoor structures, called "natural landmarks", to calibrate the results of localization or dead-reckoning [13], [32]. However, many architectural elements, like elevators, escalators, and stairs, are sparsely deployed, thus having limited help for improved localization accuracy of IPSes [40].

Among all natural landmarks, doors are much more pervasive with a high deployment density in most indoor environments [29], [30]. They connect rooms and corridors, rooms and rooms, as well as corridors and staircases. Doors on existing floor plans make more contributions for the calibration of navigation paths, the correction of human locations, and the reduction of accumulation errors. For example, as shown in Fig. 1a, when a user equipped with a smartphone walks through a door, the sensors of the smartphone can be used to detect the door event automatically. And then, the accurate door position achieved from the floor plan can be utilized to calibrate the accumulation errors of IPSes, such as the dead-reckoning [31]. Hence, accurate door event detection can play an important role in dead-reckoning-based IPS and indoor navigation systems [17].

Various state-of-the-art door event detection approaches have been proposed. Vision-based approaches rely on complicated image processing and pattern recognition algorithms to identify doors [42], but are sensitive to light and picture quality. Meanwhile, infrastructure-based approaches are proposed for precise door event detection. For example, WiFi-based door event detection approaches rely on pre-installed AP infrastructures with enormous device and management cost [17]; Behavior-based door event detection utilizes the sensor information of smartphones, but is affected by complex and random users' behaviors, causing unstable detection results [24], [45]; Acoustic-based door event detection is related to the states of the door and sensitive to the surrounding noise [20]. The pre-installed infrastructures incur non-trivial, sometimes even enormous device or management cost. Therefore, these existing approaches are limited in certain applicable scenarios or conditions.

In this paper, we propose a novel light-weight magnetic-based door event detection named LMDD, which is an infrastructure-free and widely applicable approach based on popular smartphones. First, it analyzes readings from the built-in magnetic sensor of a popular smartphone [23], [29]. The anomalies or sharp fluctuations of magnetic signals are captured after complex environmental noises and

- *L. Gong is with the School of Software and BNRist, Tsinghua University, Beijing 100084, China, and the School of Computer Science and Engineering, Tianjin University of Technology, Tianjin 300384, China. E-mail: gongliangyi@gmail.com.*
- *Y. Zhao is with the AI Labs, Simple Educational Corporation, Beijing 100191, China. E-mail: zhaoyiyang@gmail.com.*
- *C. Xiang is with the College of Computer Science, Chongqing University, Chongqing 400044, China, and the Army Logistics University of PLA, Chongqing 401311, China. E-mail: xiang.chaocan@gmail.com.*
- *Z. Li is with the School of Software and BNRist, Tsinghua University, Beijing 100084, China. E-mail: lizhenhua1983@gmail.com.*
- *C. Qian is with the Department of Computer Engineering, University of California, Santa Cruz, CA 95064. E-mail: cqian12@ucsc.edu.*
- *P. Yang is with the School of Computer Science and Technology, University of Science and Technology of China, Hefei, Anhui 230026, China. E-mail: panlongyang@gmail.com.*

Manuscript received 21 Sept. 2016; revised 9 Sept. 2018; accepted 12 Oct. 2018. Date of publication 18 Oct. 2018; date of current version 30 Sept. 2019. (Corresponding author: Chaocan Xiang.)
For information on obtaining reprints of this article, please send e-mail to: reprints@ieee.org, and reference the Digital Object Identifier below.
Digital Object Identifier no. 10.1109/TMC.2018.2876841

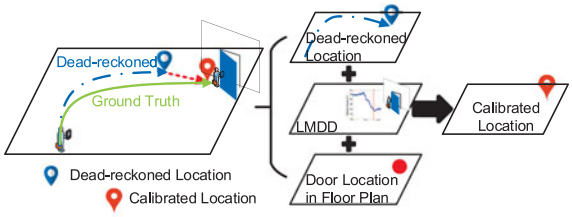

(a) Usage example of indoor localization based on LMDD

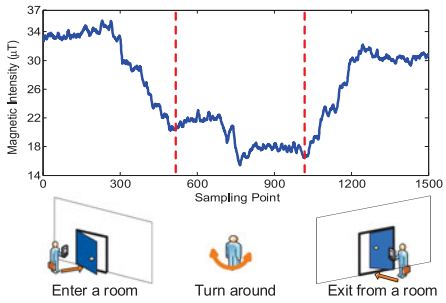

(b) Changes of magnetic intensity across sampling points.

Fig. 1. The usage scenario of LMDD in Indoor Positioning Systems (IPSes) and its basic idea based on the magnetic intensity change.

random measurement noises are wiped. Then, door-passing events are detected by applying probability-based Bayesian techniques. The exciting thing is that extensive experiments demonstrate door-passing events can be passively and efficiently detected by magnetic sensing data without any pre-installed infrastructure, as demonstrated in Fig. 1b.

The biggest challenge of LMDD is to accurately extract the signal features for a door-passing event. This is because magnetic signal fluctuations may be caused by various unexpected "environmental events". For instance, magnetic intensity values also change sharply when the holder shakes the smartphone. To eliminate such "noises" (i.e., denoising), we combine a feature analysis algorithm with automatic filtering on magnetic sensing data in LMDD.

Moreover, we explore how to substantially improve the performance of LMDD by human activity analysis and context awareness with non-magnetic built-in sensors. We perform extensive experiments and find that only four sensors, i.e., gyroscope, accelerometer, light sensor, and WiFi receiver, can be practically used for improved door event detection. But each of four sensors is only good at one specific type of application scenarios. In order to enhance the robustness and accuracy of door event detection, we propose a fusion method of heterogeneous sensors data based on a majority-voting model.

We have implemented a prototype of LMDD and successfully deployed it on multiple popular Android phones, including Google Nexus 5, Samsung Galaxy S4 and HTC One M8 etc. We evaluate the performance of LMDD in five typical environments, including offices, classrooms in a university, residential houses, a hospital and a laboratory. Experimental results show that the door event detection accuracy of LMDD is around 80 percent on average, ranging from 70 to 87 percent. Meanwhile, the computational complexity of LMDD is in $O(KN{\sigma_s}^2)$, where K denotes the number of doors, N represents the necessary sampling points for detecting a door, and σ_s is the width of the Gaussian function. The enhanced LMDD based on the fusion of heterogeneous sensors can be increased to an average of 90 percent, ranging from 88 to 93 percent, which is taken as a generally satisfactory level in practice.

The main contributions of our work are listed as follows:

- We propose LMDD, a novel light-weight magnetic-based door event detection without any pre-installed facility. LMDD only relies on natural magnetic feature information collected from common smartphones. It can achieve accurate door event detection by data acquisition, events identification and events denoising.
- We further propose an improved and robust door event detection framework based on a majority-voting model to fuse multiple-dimensional sensing data from four heterogeneous sensors.
- We have implemented a prototype of LMDD and deployed it on multiple popular Android phones. Experimental results show that the door event detection accuracy of basic LMDD is up to 80 percent on average, which proves the effectiveness of LMDD. Moreover, the enhanced LMDD based on the fusion of heterogeneous sensors can further increase the accuracy to 90 percent on average.

Roadmap. The rest of this paper is organized as follows. First, we survey related work in Section 2. Then, we introduce the design of LMDD in Section 3. After that, we present the improved schemes that optimize the performance of LMDD in Section 4. We describe the system implementation and report evaluation results in Section 5. In the Section 6, we discuss five factors that affects the performance of LMDD and also propose the potential solution to improve the performance. Finally, we conclude our work in Section 7.

2 Related Work

In most of current researches, dead-reckoning-based IPS is considered as the most popular method in indoor navigation due to greatly less labor cost [19], [38], compared with the fingerprinting-based IPS. The dead-reckoning mainly employs landmarks on a floor plan to calibrate the positions so as to improve localization accuracy. The door is one of the most important and popular landmarks in the indoor environments [31]. As a result, the door event detection, which is key to improved indoor localization or navigation, is widely studied in recent years [40]. The existing works of door event detection are mainly comprised of two categories: vision-based approaches, infrastructure-based approaches.

1) *Vision-Based Approaches.* With the help of cameras, doors can be recognized by image processing and pattern recognition in terms of specific shapes, colors, scales, and textures. A boosting algorithm [15] was introduced to classify doors in various environments. Structures of doors become weak classifiers, such as frames, knobs, hinges and gaps. Doors are determined by a strong classifier that is the weighted summation of all weak classifiers. Specifically, a probabilistic framework based on door models was proposed [3]. Comparing with modeling data in a database, doors are identified with at least 84 percent confidence. Context information [9], [11] was also introduced to distinguish doors with different functions, such as exits, restrooms and offices. However, the complex indoor scenarios, such as the dark [18] or the imprecise photographing angle [19], [39], may affect the quality of pictures taken on the smartphones [25], [39], [41], decreasing the accuracy and applicability of vision-based approach.

2) *Infrastructure-Based Approaches*. Yang et al. [16], [40], [42] employ pre-deployed infrastructures to do indoor localization, such as WiFi and ultrasound sensors. When positions of tracking objects are obtained, locations of doors can be found or calculated. Specifically, Hnat et al. [16] proposed a tracking scheme called "Doorjamb", which uses many ultrasound sensors on doors to detect moving objects. Yang et al. [40] proposed a novel indoor localization called "LiFS" based on WiFi infrastructures. In the LiFS, doors are treated as key reference points to establish the relationships between stress-free floor plan and fingerprint space. And then, door detection is achieved by comparing with the RSS values near doors. UnLoc [31] was proposed as an unsupervised indoor localization based on sensor-based dead-reckoning and environment sensing. It uses seed landmarks to re-calibrate human locations, thus requiring no site survey and no installation of additional infrastructures except WiFi. In the UnLoc, the door detection relies on the surrounding abundant WiFi APs, which is less dependable/scalable. Besides, infrastructure-based methods suffer from the limited coverage, expensive system costs and unstable signal strengths.

In summary, all current works of door event detection are based on either vision or pre-install infrastructures. They incur enormous cost and are sensitive to applicable environments, which impairs the universality and usability of door event detection in the IPS systems. To overcome this deficiency, we explore how to leverage the magnetic information to achieve pervasive and accurate door event detection with the following two reasons [44]. First, as the earth magnetic field exists almost everywhere in the world, LMDD can be applicable to nearly all the kinds of environments. Moreover, the natural magnetic information is easy-access in common smartphones, and insensitive to users' behavior and severe environments (dark, secret, noisy, etc. expect metal objects) [41]. As a result, LMDD can achieve an accurate and robust door event detection.

3 Methodology

In its basic design, LMDD is a door event detection approach that only relies on the sensing data from a single smartphone. It utilizes the magnetic field characteristics (Section 3.1) to realize the *door event detection that refers to detecting the event whether a user is passing through a door or not*. The approach consists of three processes: data acquisition (Section 3.2), events identification (Section 3.3), and environmental event cancellation (or called denoising (Section 3.4).

3.1 Magnetic Field Characteristics

In general, the magnetic field observed by sensors is a combination of 1) geomagnetic field and 2) ambient magnetic field. The geomagnetic field (i.e., the magnetic field of the earth) often acts as a global reference for orientation detection and navigation. However, magnetic interferences in the indoor environment cause that the geomagnetic field fails to report right directions. Non-uniform distributions of magnetic fields inside buildings directly affect electric compass [12]. To understand the changes of magnetic signals near the door area, we investigate the influence of building structures and the trend of magnetic characteristics under different cases.

3.1.1 Features of Magnetic Field Near a Door

Modern buildings usually have many electronic and ferromagnetic structures, such as reinforced concrete, electronic sub-systems, and metallic furniture. These ambient magnetic fields may well cause magnetic anomalies in certain areas [10]. A typical example is shown in Fig. 2. The wall of a room is made of reinforced concrete or steel structures, which can obviously affect indoor magnetic field distributions like a metallic box. Thus, the magnetic field inside the room is different from that outside the room, e.g., in the corridor.

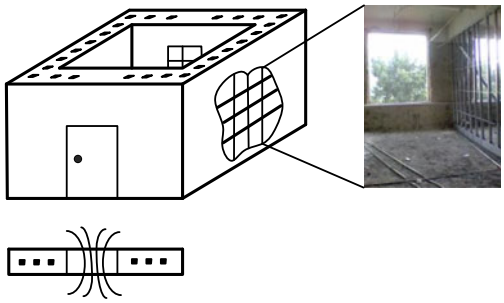

Fig. 2. The structure of a modern room and the door.

Generally speaking, distributions of magnetic fields in distinct parts of a building are quite different [14]. Since doors are usually the breaking parts of reinforced concrete or steel walls, the magnetic intensity changes drastically on both sides of a door. Meanwhile, doors often contain a few metallic components, such as doorknobs, hinges, and metal panels, thus interfering the readings of the magnetic sensor. In a nutshell, doors are the boundaries of two major zones of modern buildings, i.e., rooms and corridors, so sharp changes of magnetic intensity are taken as the hints of doors.

3.1.2 Trend of Magnetic Field for Different Cases

For obtaining magnetic distributions inside a building, we conduct a series of benchmark experiments using a typical magnetic sensor (Honeywell HMC5883L). First, we measure the magnetic intensity when holding the device in a fixed position. The result is plotted in Fig. 3a, demonstrating the stability of magnetic intensity in a fixed position. Then, the holder walks along a straight corridor, and the result is shown in Fig. 3b. In this case, it is hard to identify obvious features from the changes of magnetic intensity. Finally, the holder passes through a door and walks into a corridor, and the result is recorded in Fig. 3c. Obviously, there is a clear "drop and rise" pattern in Fig. 3c, which implies the event of passing through a door.

3.2 Data Acquisition

Most of today's smartphones contain magnetometers or compasses for providing navigation services. The output of these sensors consists of three vector components in x, y and z axes. It has been reported that a smartphone is in most time horizontally placed [28]. So, when people use smartphones for indoor navigation, the x and y axes compose the horizontal plane and the z axis represents the vertical direction.

A magnetic sample at time t is made up of three components $\{M(x), M(y), M(z)\}$. Each component represents the reading of an axis. Let M denote the square root of the magnetic fields of all three vectors, so $M = \sqrt{M(x)^2 + M(y)^2 + M(z)^2}$. Then, the azimuth angle ψ can be calculated as

$$\psi = \arctan \frac{|M(z)|}{\sqrt{M(x)^2 + M(y)^2}}. \quad (1)$$

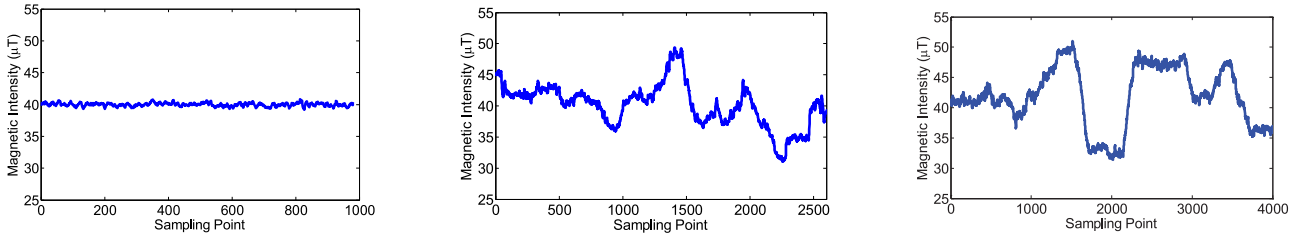

(a) In a fixed position (b) In a corridor (c) In a corridor with a door

Fig. 3. Magnetic intensity samples in three situations.

Normally, the magnetic sensors are often assembled on the board of a smartphone. During the sensing period, carrying ways of the smartphone are changed frequently. Thus, the spatial posture of the magnetometer must be considered. In addition to the azimuth angle ψ, the pitch angle ω and the roll angle θ are introduced to determine the spatial posture. The pitch angle controls the relative elevation between phone and horizontal plane and the roll angle refers to the rotation around the X direction respectively. We can transform the onboard coordinate system (OCS) to the local absolute coordinate system (LACS). Fig. 4 elaborates three angles in the transformation between OCS and LACS. All magnetic intensities of our approach are obtained in LACS. Hence, the influence of the spatial posture is limited to a minimum level according to the results of transformation of the coordinate systems. Three components of the magnetic strength in LACS can be derived as follows:

$$M_L = A_\psi \cdot A_\omega \cdot A_\theta \cdot M_O, \tag{2}$$

where M_L represents the magnetic components in LACS and M_O represents the magnetic components in the onboard coordinate system respectively. The arrays of three angles are shown as follows:

$$A_\psi = \begin{bmatrix} \cos\psi & \sin\psi & 0 \\ -\sin\psi & \cos\psi & 0 \\ 0 & 0 & 1 \end{bmatrix}$$
$$A_\omega = \begin{bmatrix} 1 & 0 & 0 \\ 0 & \cos\omega & \sin\omega \\ 0 & -\sin\omega & \cos\omega \end{bmatrix} \tag{3}$$
$$A_\theta = \begin{bmatrix} \cos\theta & 0 & -\sin\theta \\ 0 & 1 & 0 \\ \sin\theta & 0 & \cos\theta \end{bmatrix}.$$

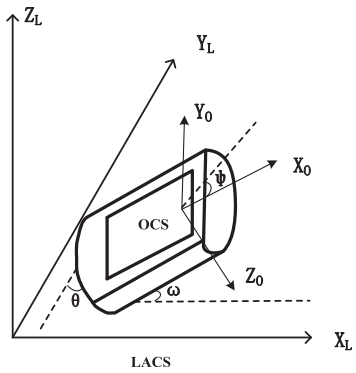

Fig. 4. The relationship between OCS and LACS.

For simplicity, we still use M to denote the M_L in the remaining sections. The magnetic intensity can be calculated from three magnetic components. After the translation from OCS to LACS, the effect of smartphone postures is reduced to the minimum level. Therefore, sensing data traces from different participators have the same evaluation base. When people use smartphone to do indoor navigation, the smart phone is faced up with a high probability [28]. Hence, we assume that the smart phone is placed in parallel to the ground during the trace collection phase. It means that the Z component is stable unless the metal materials appears in the vertical direction. Therefore, we can use the magnetic strength directly to represent the magnetic trace.

3.3 Events Identification

As plotted in Fig. 5, LMDD identifies door events in four steps: 1) pre-processing, 2) denoising, 3) feature definition, and 4) event reporting. First of all, pre-processing eliminates Gaussian white noise from raw data and helps to improve the data accuracy. In the second step (denoising), we propose an edge preserving filter to wipe out random measurement noises, so that the anomalies or sharp fluctuations of magnetic signals become clearer. In the third step (feature definition), we use a Bayes function based on empirical feature classifications to regenerate the signal. Finally, the door events are identified based on a priori threshold in the event reporting.

Let K denote the number of potential doors, N represent the necessary sampling points for detecting a single door (typically between 100 and 200), and σ_s denote the width of the Gaussian function (typically between 20 and 100), it is easy to prove that the computation complexity of LMDD stays in $O(KN{\sigma_s}^2)$. This means that our algorithm only concerns those sharp changes within a short time.

3.3.1 The Edge Preserving Filter

The raw data of magnetic intensity on each axis (say x) collected by a sensor can be represented as

$$M(x) = M_{bh}(x) + M_n(x) + M_e(x), \tag{4}$$

where M_{bh} is the basic harmonic determined by the geomagnetic intensity, M_n is the magnetic intensity of noise signal, and M_e is the magnetic intensity of environmental signal. $M_n(x) + M_e(x)$ denotes the intensity of ambient magnetic fields.

According to human route analysis and our experiments, when a person passes through a door, his/her moving direction does not change. Hence, M_{bh} should be stable and consistent to the values before and after the door event.

The noise signal M_n contains inevitable Gaussian white noises and random measurement noises. Gaussian white noises lead to the small jitter of signals that may harm the

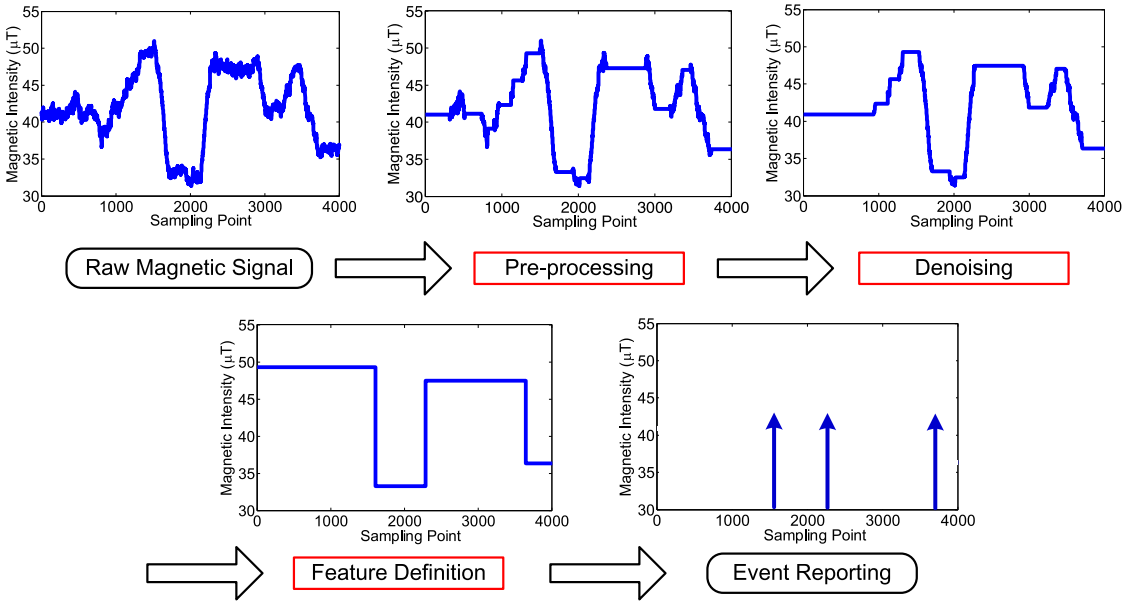

Fig. 5. The outline of signal analysis procedures.

detection accuracy, while random measurement noises induce serious shaking of signals in the time domain [43]. As illustrated in Fig. 3c, the magnetic intensity is supposed to go down or up gradually (smoothly), but in practice it shakes seriously due to the random measurement noises. In order to improve the accuracy of door event detection, it is necessary to remove noises and to smooth the signal curves while preserving the edges of changed signals.

Algorithm 1. Edge Preserving Algorithm $F[M]_p$

Input: A data trace, M_n, and the total number of sampling points, T;
Output: The filtered trace, M_{nn};

```
1) Set a window size S, where S ≤ 2σ_s.
2) For p in T
3)   Initialize: N_p = 0, F_p = 0;
4)   For q ∈ [p − S/2, p + S/2]
5)     m = G_σs(‖ p − q ‖)G_σr(‖ M(p) − M(q) ‖);
6)     F_p += mM(q);
7)     N_p += m;
8)     Standardization M_nn = F_p/N_p;
9)   End For
10) End For
11) Return M_nn
```

To this end, we first use empirical values to calibrate the built-in magnetometers. Afterwards, we design an edge preserving filter $F[M]_p$ (p is a sampling point) to remove those random measurement noises. Meanwhile, we make efforts to preserve the boundaries, spikes, and canyons of signal curves [22]. Specifically, the edge preserving filter is constructed based on a linear Gaussian filter that utilizes the position-dependent renormalization

$$G_{\sigma_s}M(p) = \frac{1}{N_p}\sum_{q\in S} G_{\sigma_s}(\| p-q \|)M(q). \tag{5}$$

Here, because the noise distribution of magnetic signals approximates the Gaussian distribution, we leverage the Gaussian function as the weight $\omega = G_{\sigma_r}$ when there seems to be an edge between p and q. The bigger $||M(q) - M(p)||$ is, the more probable there is an edge between p and q [22]. Thereby, the edge preserving filter is generated as follows:

$$F[M]_p = \frac{1}{N_p}\sum_{q\in S} G_{\sigma_s}(\| p-q \|)G_{\sigma_r}(\| M(p)-M(q) \|)M(q), \tag{6}$$

where S is the linear area centered in p in the x-axis, and N_p is the normalization factor

$$N_p = \sum_{q\in S} G_{\sigma_s}(\| p-q \|)G_{\sigma_r}(\| M(p)-M(q) \|). \tag{7}$$

Here G_{σ_s} is a spatial Gaussian kernel and G_{σ_r} is a range Gaussian kernel [5]. The normal "$\| \cdots \|$" represents the euclidean distance. Shown in Fig. 9, the spatial Gaussian kernel means the time interval between p and q. Typically, the q is in a range such that $\| p-q \| \leq \sigma_s$. The range kernel gives the difference of magnetic intensities. The parameter σ_r controls the edge preservation effect. Those kernels can be calculated as follows:

$$\begin{aligned} G_{\sigma_s}(x) &= \frac{1}{2\pi{\sigma_s}^2} exp\left(-\frac{x^2}{2{\sigma_s}^2}\right) \\ G_{\sigma_r}(y) &= \frac{1}{2\pi{\sigma_r}^2} exp\left(-\frac{y^2}{2{\sigma_r}^2}\right), \end{aligned} \tag{8}$$

where σ_s and σ_r are adjustable constants, which are determined by the analysis of empirical results. The spatial parameter σ_s decides the range features in the time domain, i.e., the width of sampling points. At the same time, the magnetic difference is scaled by σ_r. The pseudo-code of the filter is illustrated as Algorithm 1.

After applying the edge preserving filter, periodic noises and Gaussian white noises were eliminated from the magnetic signal. Comparing with straightforward Gaussian Blur algorithms, our improved bilateral filter not only considers the amplitude of magnetic strengths but also deliberates the time intervals of signal. Therefore, the variation of magnetic intensities is regarded to preserve edges. The

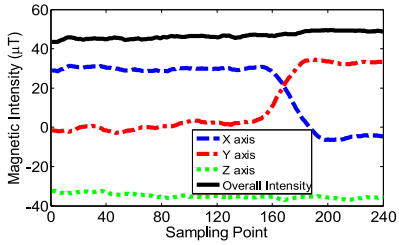

Fig. 6. Changes of magnetic intensities when the holder turns around.

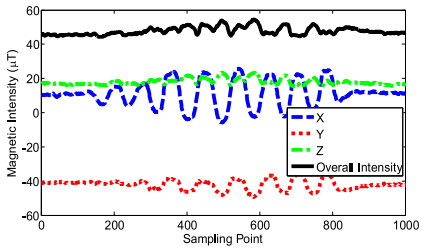

Fig. 7. Changes of magnetic intensities when the holder shakes body.

accuracy and efficiency of the signal processing is enhanced conspicuously.

3.3.2 The Bayes Function

The change of the environmental signal M_e reflects environmental events in two major types: *human activities* and *passive events*. Human activities are the phone holder's actions, such as turning around, body shaking, and shaking the phone. They are basically unpredictable. To understand the impact of human activities, detailed feature analysis on signal changes is needed. We use p_{ea} to denote the probability of human activities in all magnetic samples.

On the other hand, passive events represent ambient magnetic changes caused by environmental events, which include the sharp changes in one axis or two axes of the magnetometer. We use p_{ee} to denote the probability of passive events in magnetic samples.

Our concerned door events belong to the passive events, and the process of door event detection is based on the computation of probability. Specifically, we use $p(d)$ to denote the ratio of door events among all passive events. Accordingly, we use $\mathrm{p}(\bar{d})$ to denote the ratio of the other passive events, which may be caused by people's moving towards metal material or electrical devices.

Formally, given the magnetic changes, the conditional probability of the door event is calculated based on prior knowledge from the measurements of indoor positioning systems as follows:

$$p(d|em) = \frac{p(em|d) \cdot p(d)}{p(em)}, \tag{9}$$

where $p(em) = p_{ea} + p_{ee}$ is the measurement of all environmental events. $p(em)$ can be calculated as follows:

$$p(em) = \sum_{i=1}^{n} p(em)_i \tag{10}$$

$$p(em)_i = p(em_i|d) \cdot p(d) + p(em_i|\bar{d}) \cdot p(\bar{d}), \tag{11}$$

where n is the number of distinct environmental events and i is the event index. The parameter $p(em)_i$ represents the probability of the ith event among environmental events. It

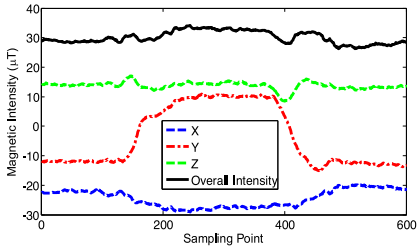

Fig. 8. Changes of magnetic intensity when the holder is close to metallic material.

is difficult to list all possible $p(em)_i$. We only describe three cases. For example, the probability of turn-around events $p(em)_1$ is the number of turning around events divided by the number of all environmental events.

Obviously, $p(em)_1$ is a part of p_{ea}, caused by human activities. Similarly, the probability of shaking body event $p(em)_2$ is the number of shaking body events divided by the number of all environmental events. $p(em)_2$ also belongs to the probability p_{ea}. Accordingly, the probability of approaching metals $p(em)_3$ is retained in the probability p_{ee} [6].

We employ $p(d|em)$ as the estimator to determine the door events. If $p(d|em)$ is greater than a given threshold ε (a constant value based on prior knowledge), a door event is detected. To understand the threshold ε clearly, below we provide an example. If the door appears after a turn-around event, ε exceeds the threshold obviously. It means that the door event is very likely to be connected with the turn-around event, since most doors are located in one side of the corridor.

3.4 Environmental Event Cancellation (or Event Denoising)

Door event detection results based on signal analysis may involve false positives, due to environmental events that are not essentially related to doors. For more accurately defined features, more detailed signal features of magnetometers need to be investigated. For example, if metal material appears on a side of the sensing area, readings from one axis (x or y) would change (but readings from the z axis are not affected). Signal changes by human activities also have specific patterns. Fig. 6 shows the change pattern of three axes when a man makes a 90 degree turn. Obviously, the average magnetic intensity almost keeps in the same value, but the values of x-axis and y-axis seem "exchanged". When the man carrying a smartphone walks slowly and shake their body, the pattern is illustrated as Fig. 7. If the smartphone holder moves to near a metallic object, the pattern is sketched in Fig. 8.

The features of common environmental events can be formally described. If we define the features with specific functions well, the irregularities and periodic noises like body shaking and turning back can be observed and excluded from event reports. A critical observation lies in that the metal material near the door area only affects one or two plain axes (e.g., x-axis or y-axis) of the magnetometer. Consequently, LMDD utilizes the following cross correlative function to search positive activities

$$C_{xy} = \frac{\sum_{i=1}^{n}(M(x)_i - E(M(x)))(M(y)_i - E(M(y)))}{\sqrt{\sum_{i=1}^{n}(M(x)_i - E(M(x)))^2 \cdot \sum_{i=1}^{n}(M(y)_i - E(M(y)))^2}}, \tag{12}$$

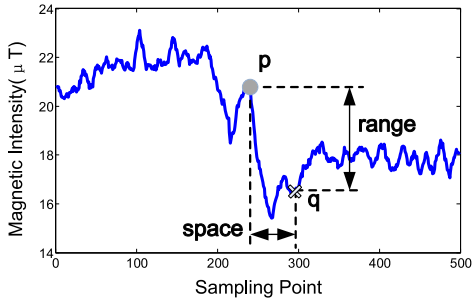

Fig. 9. The spatial and range Gaussian kernels.

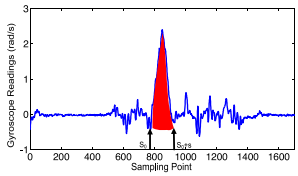

Fig. 10. Changes of the gyroscope readings when passing through a door.

where $E(M(x))$ and $E(M(y))$ are the expected values of magnetic intensity. The cross correlation C_{xy} ranges from 0 to 1.0. The larger $|C_{xy}|$ is, the higher the correlation between the events is. When $|C_{xy}|$ exceeds a threshold ξ, LMDD filters this event from the results. In the LMDD, the events are divided into three kinds: 1) highly relevant events, 2) correlated events, and 3) weakly relevant events. In order to denoise undesirable events and avoid possible loss of detection accuracy, the threshold is chosen in the range interval of correlated events according to priori knowledge of indoor positioning systems. According to our experiments, for highly relevant environmental events, ξ is larger than 0.8. If ξ lies between 0.5 and 0.8, those events are treated as "correlated events". Other kinds of environmental events are identified in the similar way.

4 Heterogeneous Sensors Fusion

Although LMDD can only use magnetic information to achieve the door event detection, its accuracy and robustness are limited by the complex influence of indoor surroundings and the low precision of available magnetic sensors, which will be discussed in Section 6. Specially, the complex indoor surroundings have many various large metal objects that affect the magnetic information. For example, when a smartphone is close to metal household appliances or metal furniture, the readings of the built-in magnetic sensor will change erratically. Thus, it is extremely difficult to only use the non-infrastructure-based magnetic information to achieve highly accurate door event detection. Even worse, the magnetic sensors built in the commercial smartphones are inaccurate and vulnerable to noise due to their low costs, hence high-precision door event detection is almost impossible without particular devices equipped with high-performance magnetic sensors. As a result, to address this problem, we explore to utilize human activity analysis and context awareness with other built-in sensors of commercial smartphones to further improve detection performance as follows.

4.1 Non-Magnetic Sensor Based Door Event Detection

According to our survey, most of commercial smartphones are mainly equipped with gyroscope, accelerometer, WiFi receiver, barometer, proximity sensor and light sensor, besides magnetic sensor [41]. Obviously, both the barometer and the proximity sensor are irrelevant to the door event detection [31]. As a result, we conduct extensive experiments to investigate whether the other four sensors can be utilized to further improve the detection performance of LMDD. In these experiments, we carry an Android-based phone to walk through 30 doors of three different kinds in four typical environments, including office, classroom, residential house and hospital. Moreover, we collect about 1,200 samples of Gyroscope, Accelerometer, Light Sensor and WiFi Receiver for door event detection, and the experimental results are specified as follows.

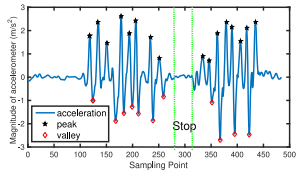

Fig. 11. Changes of the acceleration readings when passing through a closed door.

1) Gyroscope. As shown in Fig. 1b, when a user walks into a room from a corridor, s/he often changes the walking direction and turns into the door [45]. As shown in Fig. 10, this turn can lead to a large rotation angle of the smartphone, which is useful to identify the door event detection based on the changes of gyroscope data. Hence, we can detect the door-passing event according to this rotation angle which can be calculated based on the gyroscope readings as follows.

As the readings of the digital gyroscope in a smartphone are discrete, we approximately calculate the angle of human rotation by summarizing the gyroscope samples within a certain time interval. Specifically, the rotation angle of the smartphone denoted by W can be computed as

$$W = \int_{T_0}^{T_0+t} \nu(t)\, dt \approx \sum_{i=S_0}^{S_0+s} \nu_i T_i, \tag{13}$$

where T_0 is the starting time of a revolving action, and t is the duration of the rotation. We use i to represent a discrete sampling point, which is started from S_0 to $S_0 + s$ during walking through a door. ν_i and T_i denote the angular velocity and the elapsed time at the ith sampling point, respectively. Both of them can be obtained from the smartphones, such as the gyroscope readings ν_i.

According to Eq. (13), we can compute the rotation angle W based on the gyroscope readings through integrations, like the red part in Fig. 10. If the W is larger than a pre-set threshold γ_g, it indicates that the user may walk through a door. According to our experiments, when the door is open, γ_g is at least 1.7 within $2s$ time window, while it is above 1.7 within $4s$ time window when the door is closed.

2) Accelerometer. Similar to Gyroscope, the profile of the accelerometer data has a distinguished feature when the user walks through a closed door. Specifically, as shown in Fig. 11, the accelerometer data changes greatly at the first, then becomes stable, finally varies significantly again. Intuitively, when a person passes through a closed door, she/he first would walk to the door, followed by stopping moving to open it, then continue to pass through this door. As a result, it is feasible to infer whether a person walks through a door by identify the movement pattern, i.e., moving-stop-moving [1].

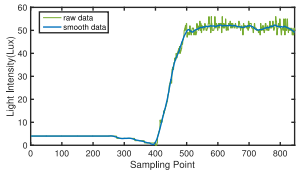

Fig. 12. Changes of the light intensity when passing through a door.

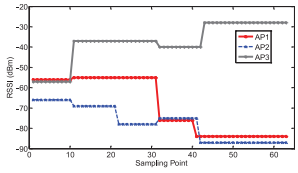

Fig. 13. Changes of the WiFi signal strengths when passing through a door.

In the following, we use the accelerometer data to count the movement steps, which are used to infer the movement status.

In our experiments, we employ a lightweight and practical step counting algorithm that utilizes the time-varying magnitude of acceleration, as shown in Fig. 11. In order to alleviate the influence of random noise, we first composite three triaxial data of the accelerometer and adopt $a = \sqrt{x^2 + y^2 + z^2}$ as the magnitude of acceleration. Then, the savitzky-golay filter [26] is employed to smooth the data curve after the static component is removed. Finally, the peaks and valleys are detected based on the pre-set thresholds. The number of steps S is counted as

$$S = \frac{|n_p| + |n_v|}{2}, \tag{14}$$

where n_p and n_v represent the number of the peak and the valley in a time window. The number of steps S is approximatively equal to the number of peak-valley pairs.

3) Light Sensor. As shown in Fig. 12, when a person walks through a door from a corridor to enter into a room, the intensity of light sensor data changes drastically, e.g., the increase is up to 50 Lux in Fig. 12. The reasons are specified as follows. According to the observations of our experiments, the light intensities of different rooms or corridors are generally different, while the doors are the main connectors among them. Thus, we can detect the change of light intensity for the door event detection with the following method.

We first use the savitzky-golay filter to smooth the curve of light data, then calculate the mean μ_l of the light intensity in a sliding time window. If the difference of μ_l in two adjacent time windows is greater than a threshold γ_l , a door event is identified: $\mu_l(t) - \mu_l(t-1) > \gamma_l$, where $\mu(t)$ denotes the mean of light intensity in the tth time window.

4) WiFi Receiver. Although it is extremely difficult to guarantee there are large numbers of APs deployed in each doors of each buildings, it is common and popular to deploy a few sparse WiFi APs in the modern buildings [47]. For example, in our experimental environment, we found three deployed APs, which can provide the opportunity to improve the accuracy of door event detection. As illustrated in Fig. 13, the RSSI values of the smartphone for all the three APs change substantially when the person passes through a door, i.e., around the 40th sampling point. As a result, we can use these WiFi APs to detect the door as follows.

We first compute the change of the average RSSI values in two adjacent time periods for each WiFi AP. If the change of the ith WiFi AP is greater than the threshold γ_{ap}, a door event is detected ($\psi_i = 1$), otherwise it is not detected ($\psi_i = 0$). The experimental results show that γ_{ap} is set 10-20 dBm, as the strength of WiFi signal would exhibit obvious difference (e.g., around 10-20 dBm) on both sides of a wall. Finally, we fuse the decision results of all the WiFi APs to reduce the false positive.

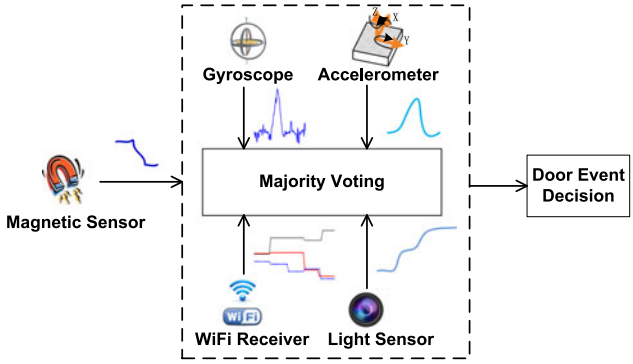

Fig. 14. The framework of door event detection based on the fusion of heterogeneous sensor data.

4.2 Fusion of Heterogeneous Sensor Data

The above experimental observations and analysis show that Gyroscope, Accelerometer, light sensor and WiFi receiver of smartphones can be used for door event detection. Nevertheless, each sensor is only good at a specific kind of scenarios in terms of the detection accuracy, due to their different dimensional sensing data [7]. For example, the precision of gyroscope-based door event detection is high when a person passes through a door with a big turn; accelerometer-based door event detection is accurate when passing through the closed doors; light-based door event detection works well when the light intensity is different between a room and a corridor; the good performance of WiFi-based door event detection highly depends on large numbers of deployed APs in the environment. Due to the diverse and complex indoor surroundings, the single-dimensional sensing data is not enough for door event detection when only using any one of these four sensors. As a result, we fuse multiple-dimensional sensing data from four different sensors to improve the robustness and accuracy of door event detection.

Specifically, Fig. 14 illustrates the framework of door event detection based on the fusion of multiple-dimensional sensing data. First, we detect this door-passing event only based on the magnetic sensing data. If the result indicates that it may be true, it will continue confirming its truth by fusing the detection results of other four sensors, or no door event is detected. In our method, as Eq. (15), we use weight-based majority voting scheme for the fusion, in order to differentiate the contributions of different sensors to the door event detection

$$V = \sum_{i=1}^{N} \omega_i r_i, \tag{15}$$

where N is the number of built-in sensors. r_i denotes the detection result of ith sensor, where $r_i = 1$ when the ith sensor reports a door-passing event, otherwise $r_i = 0$. ω_i is a priori weight based on the contribution of ith sensor to improving LMDD. If V exceeds a pre-set voting threshold κ, a door-passing event is eventually reported. Otherwise, there is no door-passing event detected.

(a) office rooms (b) the laboratory (c) the hospital (d) classrooms (e) residential house

Fig. 15. The doors of different environments.

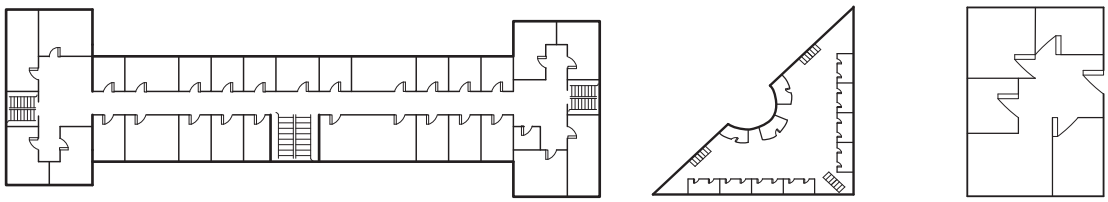

(a) The floor plan of offices (b) The floor plan of classrooms (c) The floor plan of the house

Fig. 16. Floor plans of the experimental environments.

5 Performance Evaluation

5.1 Experiment Setup and Settings

We implement a prototype system of door event detection to realize LMDD method as follows. First, we develop a smartphone App based on Android platform to collect the sensing data of the smartphone sensors, including the magnetometer, gyroscope, accelerometer, light sensor and WiFi receiver. And then, the smartphone sends the sensing data to a remote server by the Cellular network and WiFi. Finally, based on these sensing data, the server uses the LMDD method to detect whether the door exists.

As shown in Fig. 15, we make experiments in five different kinds of typical environments, including office, classroom building, residential house, hospital and laboratory. For one thing, the doors of office, hospital and laboratory are symmetrically distributed along a corridor, while the room arrangement is not regular and the directions of doors are diverse in the classrooms. For another, the doors are made of metallic material in the classroom, hospital and laboratory, nevertheless, most of doors are wooden in the office and house, while some doors are made of glass in the laboratory. The floor plans of the office, the laboratory, the hospital, and the classroom are illustrated in Fig. 16.

In the experiments, we recruit 50 volunteers who are living, working, or studying in these five environments. They use five different kinds of popular smartphones, including Samsung Galaxy S4, Huawei Ascend P7, Sony Xperia Z2, XiaoMi M2S, and Meizu MX. In total, we conduct about 1800 times of experiments in three months, where more than 100 door events are included. For each door, we collect positive data when a person holds a smartphone to walk into and out of the door, respectively. Also, we collect negative data when a person holds a smartphone to approach the wooden, the metallic and the glass objects, such as the furniture, the cookers and the fish tanks, etc.

As it is extremely difficult to use mathematical model to calculate the optimal identification threshold of door-pass event [29], we exploit the statistical analysis based on real experiments to get their parameter settings. Specifically, we made large numbers of repeated experiments, and computed the threshold value with 95 percent confidence level based on the statistical analysis. For example, the thresholds of gyroscope, accelerometer, light and WiFi are 1.7, 0.7, 46Lux and 15 dBm, respectively. Its rationality is that these threshold values can guarantee that the door identification accuracy is no less than 95 percent [21]. Further more, the more the repeated experiments, the better the threshold settings. We set the time windows 2 s for an open door and 4 s for a close door, respectively, according to the observations of our experiments. The threshold ξ of event denoising (refer to Section 3.4) is initialized as 0.7.

We mainly utilize two metrics to evaluate the door event detection performance [36], [46]: 1) false positive rate(FPR), the fraction of cases where the LMDD announces a 'Door Detected' event but a user doesn't walk through a door actually, as Eq. (16). 2) false negative rate(FNR), the fraction of cases where a user walks through a door but the LMDD fails to detect the door, as Eq. (17)

$$FPR = \frac{\sum_{j=1}^{m} FP_j}{\sum_{j=1}^{m} N_j} \tag{16}$$

$$FNR = \frac{\sum_{j=1}^{m} FN_j}{\sum_{j=1}^{m} P_j}, \tag{17}$$

where m is the number of different experimental environments. FP_j denotes the number of positive reports about false door events and FN_j denotes the number of negative reports about true door events in the jth experimental environment, respectively. P_j denotes the number of true door events and N_j denotes the number of false door events in the jth experimental environment. In this paper, we use the true positive rate (TPR) as the accuracy of door event detection in the performance evaluation of LMDD. The TPR is the percentage of true door events detected correctly [46], i.e., $TPR = 1 - FNR$.

5.2 Experiment Results

In the following, we first evaluate the performance of our method by compared with the existing works. After that,

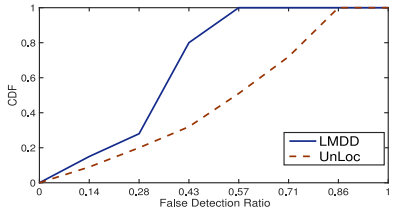

Fig. 17. Performance comparison between LMDD and UnLoc, in terms of CDF of false detection ratio.

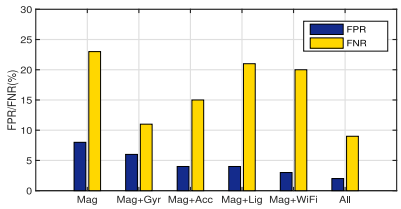

Fig. 18. The FPR/FNR of LMDD with different built-in sensors.

we evaluate the performance of our method in terms of three aspects, including various built-in sensors, experimental environments and door types. Finally, we evaluate the power consumption of our method.

5.2.1 Comparison with the State-of-the-Art

We compare our method with UnLoc [31], which uses the unsupervised learning method based on WiFi signals and Gyroscope sensing data. We conduct 100 times of experiments to detect 35 doors, and calculate the false detection ratio of all the 35 doors in each experiment. We evaluate the performance of LMDD with only magnetic sensor, by comparing its cumulative distribution function(CDF) of the false detection ratio with that of UnLoc. As shown in Fig. 17, the experimental results show that the worst false detection ration of LMDD is less than 60 percent but that of UnLoc is more than 85 percent. Besides, LMDD has the better performance with an enhancement of at least 40 percent in median false detection ratio over the UnLoc techniques. In the experiments, the UnLoc clusters on gyroscope data and WiFi together to identify turns within a WiFi area in the same cluster. The turns in the cluster are identified as doors of adjacent classrooms in a corridor. However, not every turn refers to a door, and the doors are indirectly detected in the UnLoc. In the other hand, when the number of surrounding WiFi APs decreases or the WiFi signal is weak and unstable, the detection errors of UnLoc will increase obviously, while LMDD is non-infrastructure and independent on environments. According to the above results, it can be proved that even the basic LMDD algorithm outperforms UnLoc, let alone the improved LMDD algorithms with other built-in sensors. So, by comparison, the LMDD can achieve more higher performance of door event detection.

5.2.2 The Impact of Different Sensors

In this section, we make experiments to evaluate whether the fusion of additional built-in smartphone sensors, including the gyroscope, accelerometer, light sensor and WiFi receiver, can improve the detection performance of LMDD.

First, we evaluate the influence of single sensor on the detection performance. As shown in Fig. 18, compared with the basic LMDD only based on magnetometer, it can decrease the FPR and the FNR by about 8 and 23 percent on

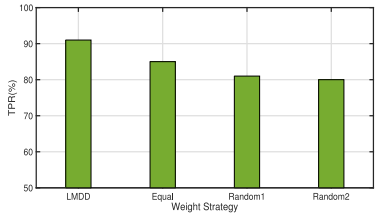

Fig. 19. The accuracy of improved door event detection with different weights combination.

average, respectively. Specifically, adding the gyroscope can achieve the FPR/FNR by about 6/11 percent and make a greatest improvement on the FNR, i.e., more than 52 percent, while adding the WiFi can achieve the FPR/FNR by about 3/20 percent and make a largest decrease of the FPR, more than 62.5 percent. Adding the accelerometer and light sensor can achieve the FPR/FNR by about 4/15 percent and 4/21 percent, respectively. We find that most doors of our experiments connect the rooms to the corridors, and a person needs to make a turn into a room from a corridor or in a reverse direction. As a result, it is very accurate to detect the doors by analyzing the change of gyroscope sensing data. Moreover, compared with the house wall, the other equipments in the house have slight impact on the RSS of WiFi signal. Thus, it is difficult to identify a non-door event as a door event by using WiFi.

Second, in the voting process, the weight of each sensor should be calculated based on the contribution of each sensor on the improved LMDD's performance [4]. The more contribution, the higher weight. Specifically, we conducted experiments and computed the contributions of each sensor based on the experimental results. For example, Fig. 18 shows that the TPRs of door event detection are increased by 12, 8, 2 and 3 percent when using gyroscope, accelerometer, light sensor and WiFi receiver, respectively. Therefore, the normalized weights of gyroscope, accelerometer, light sensor and WiFi receiver are set 0.48, 0.32, 0.08, and 0.12, respectively. Notice that, the accuracy of weight settings increases with the number of experiments. Thus, in the future, we will study how to use big data from large-scale application scenarios to further improve the accuracy of parameter settings.

In order to prove the reasonability of weight settings, we add new experiments to evaluate the performances of LMDD in different weight combinations. We compare our weight settings with other three settings, include a uniform weight (i.e., the weight of each sensor is uniformly 0.25) and two groups of random weights. As shown in Fig. 19, the performance of LMDD with our weight settings is much better than other settings. It is because our settings are based on the contribution of each sensor, where the more the contribution of each sensor, the bigger the weight. Moreover, it is an open problem to compute the optimal weight settings due to nonlinear, hard modeling contributions of these sensors [4]. In the future, we will study how to use machine learning based on a number of real experimental results to get an approximate model [7], and compute a near-optimal weight.

Finally, we evaluate the impact of the fusion of all the four built-in sensors on the detection performance of LMDD. As shown in Fig. 18, it can improve the detection performance significantly by utilizing the sensor fusion, e.g., its FPR and FNR are decreased from 8 and 23 percent to 2 and 9 percent, respectively, in comparison with the basic LMDD based on magnetometer.

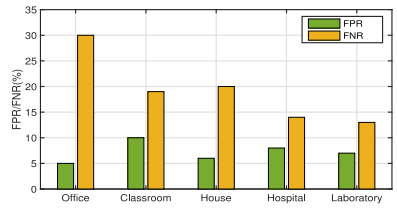

Fig. 20. The FPR/FNR of basic LMDD in five environments.

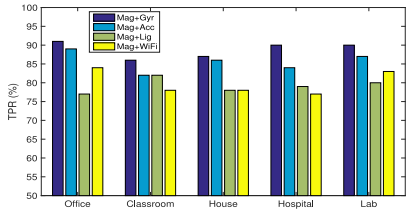

Fig. 21. The TPR of basic LMDD with different built-in sensors in five environments.

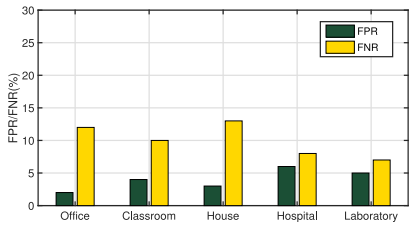

Fig. 22. The FPR/FNR of LMDD fusing all built-in sensors in five environments.

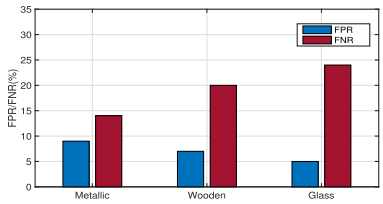

Fig. 23. The FPR/FNR of basic LMDD for three types of doors.

5.2.3 The Impact of Different Environments

We evaluate the performance of the proposed method in terms of different environments. At first, we only investigate the performance of the basic LMDD based on a magnetic sensor in five various environments: office, classroom, house, hospital, and laboratory. As shown in Fig. 20, the basic LMDD can achieve the FPR by 5, 10, 6, 8 and 7 percent and the FNR by 30, 19, 20, 14, 13 percent in the five environments, respectively. Although the performances of these five environments are similar, e.g., the differences of TPRs are less than 5 percent, the accuracy is different with the environments. Specifically, the basic LMDD can achieve the lowest FPR about 5 percent in the office and the lowest FNR about 13 percent in the laboratory. Moreover, the FPR and FNR of basic LMDD in the classroom and office are higher than those in other environments. Through analyzing the structures and layouts of environments in Figs. 15 and 16, the reasons are that the office rooms are full with massive wooden furniture (as illustrated in Fig. 15a), which makes a slight influence on the magnetic field. Thus, the FPR of LMDD in the office rooms is much lower than that of the others, while the FNR is greatly higher than the others for wooden doors. As shown in Fig. 15b, the laboratories are built well with high-density steel inside the concrete, while the doors of the laboratory connecting the rooms and the corridors are almost made of metal. As a result, it is more accurate to detect the doors and the FNR is lower than the others. However, a large number of devices with large metallic objects are deployed in the laboratory, such as electrical appliances and furniture, which affect the surrounding magnetic field seriously and incur the larger FPR. In conclusion, the performance of LMDD is different with the environments and seriously affected by the door materials, the ferromagnetic structures of buildings and the surrounding metallic objects [10], [12], [28], [31].

In order to evaluate the robustness of the identification threshold in different environments, we calculate the improvement of TPR when the magnetic-based LMDD fused each sensor in five environments. As shown in Fig. 21, the TPRs of door event detection for each sensor are increased by different levels with diverse environments, but the difference of TPRs for each sensor in five environments is small. The standard deviation of the TPRs are 2.2, 2.7, 1.9, 3.2, when basic LMDD fuses gyroscope, accelerometer, light sensor and WiFi receiver, respectively. As a result, the identification threshold of each sensor is robust, and the detection performance is relatively stable in the complex scenarios.

Moreover, we evaluate the performance of improved LMDD with the fusion of all built-in sensors in five different environments. As shown in Fig. 22, the improved LMDD can achieve the FPR by 2, 4, 3, 6 and 5 percent and the FNR by 12, 10, 13, 8, 7 percent in the five environments, respectively. The average *TPR* of door event detection is increased to 90 percent. The improved LMDD can achieve the lowest FPR about 2 percent in the office and the lowest FNR about 7 percent in the laboratory. The performance of improved LMDD in the residential house is worst with the highest FNR 13 percent because of the wooden doors and less WiFi APs. The improved LMDD performs very well in the hospital and the laboratory, where a user always needs to make a turn when he/she enters a door that is easily detected by the gyroscope and accelerometer.

In some special cases, the users may pass through the doors without turns. Thus, we evaluate whether LMDD still works without user's turns based on the experiments. We tested the performance of LMDD without the turn. The experimental results show the TPRs of LMDD with the turn and without it are 91 and 85 percent, respectively. The FNR of door event detection without the turn only increases by 6 percent, compared with that with the turn. As a result, even if the users make no turn when passing through a door, the LMDD can still achieve a good performance of door event detection with the following reasons. First, the LMDD achieves the door event detection mainly based on the magnetic field, which is nearly not affected with/without user's turn. Moreover, although the gyroscope is invalid without user's turn, the LMDD can still use the fusion of other sensors to identify the door event, thus greatly alleviating the negative influence without user's turn.

5.2.4 The Impact of Different Types of Doors

We evaluate the performance of LMDD in three different kinds of doors, including metallic doors, wooden doors, and glass doors. As shown in Fig. 23, the FNR of metallic door event detection is less than 15 percent but that of glass door event detection is more than 20 percent. Hence, it can be observed that metallic doors are more easily detected than

TABLE 1
The Power Consumption (mW) of Sensors

Parts	Average	Maximum	Minimum
Android system	151.9	215.6	88.2
Magnetometer	49	112.7	24.5
WiFi	147	245	122.5
Gyro., Acc. and Light	58.8	49	73.5

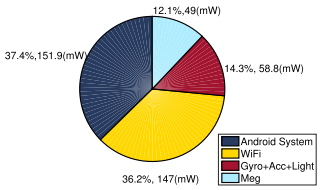

Fig. 24. The average power consumption of sensors.

others because of the serious effect of metal on the magnetic field. At the same time, in the negative experiments, when the smartphones were put near the metallic, the wooden and the glass doors, respectively, we observe that the FPR is more than 8 percent and the largest near the metallic, but is the least near the glass and only 5 percent. The FPR and FNR of wooden door event detection is only 7/20 percent. We find that the metallic doors can more easily affect the magnetic field of smartphones than the others, which is the main reason of high-accuracy metallic door event detection. Based on the above experimental observations, it can be found that the detection performances of LMDD have slight differences in various types of doors due to different materials, structure and size, which can be further leveraged to distinguish each door and benefit to indoor localization.

5.2.5 Power Consumption

In this section, we evaluate the power consumption of our method. In our system, in order to reduce the power consumption of local processing in smartphone as much as possible, we upload all sensors' data to a cloud server where all the data is processed. The energy consumption of data processing in cloud server is not included in the power consumption of smartphones. Thus, the total power consumption P_{total} of LMDD which is only related to the smartphone consists of system consumption P_{system} and sensor consumption $P_{sensors}$, i.e., $P_{total} = P_{sensors} + P_{sensors}$. The sensor consumption $P_{sensors}$ is the power consumed by the implementation of the smartphone sensors, while the system consumption P_{system} is the basic consumption of implementing the smartphone system. Then we first measure the battery level for about 100 times when only running the basic Android system, and calculate the energy consumption of Android system P_{system}. And then, in order to evaluate the power consumption of each sensor, we measure the power consumption of smartphone for 30 times when individually switching on one of WiFi, magnetometer, gyroscope, accelerometer and light sensor. Thus, we can compute the sensor consumption as $P_{sensor} = P_{total} - P_{system}$, where P_{system} is the average power consumption of Android system.

The power consumptions of Android system and various sensors are shown in Table 1. Specifically, as shown in Fig. 24, the system and WiFi consume the most energy (about 73.6 percent), where the WiFi spends the energy about 36.2 percent. Moreover, the magnetometer only uses

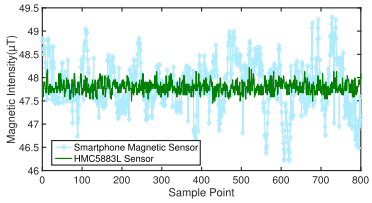

Fig. 25. Comparison between HMC5883L and smartphone magnetic sensor in the stable status.

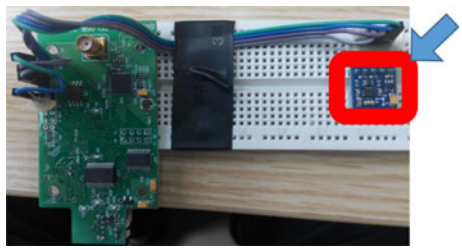

Fig. 26. The magneto-resistive magnetic sensor HMC5883L.

a small amount of energy (about 12.1 percent) while other built-in sensors consume about 14.3 percent energy. As a basic component, the Android system consumes a high amount of energy (about 37.4 percent) that is unavoidable. WiFi is another main consumer especially in the working mode, which is the other shortcoming of the UnLoc. By contrast, the energy cost of the basic LMDD with the magnetic sensors only refers to the power consumption of the system and magnetic, but UnLoc needs the 88 percent power consumption of the system, WiFi and gyroscope. The power consumption of UnLoc is seven times more than that of basic LMDD. As a result, the experimental results show that LMDD is a lightweight, low-cost and ubiquitous door event detection system.

6 Discussion and Future Work

In this section, we make extensive experiments to explore the influences of four factors on the detection performance, including the errors of magnetic sensor, the influence of users' behavior, the interference of indoor environments, the crowdsensing of massive users, and the usage of LMDD in IPSes. Further, we give the future work based on these experimental results and analysis.

Error of Magnetometer. We evaluate the error of magnetic sensor in the smartphone by comparing with a particular, accurate sensor, i.e., Honeywell HMC5883L with 5 milligauss precision [48]. As shown in Fig. 26, we connect this magneto-resistive magnetic sensor to a TelosB wireless sensor for communication, while using a laptop based on Ubuntu system to receive the magnetic sensing data. We compare the HMC5883L sensor with the smartphone magnetic sensor in terms of stable status. As shown in Fig. 25, the readings of HMC5883L is more stable than that of a smartphone magnetic sensor in the stable status, while the reading change of HMC5883L is larger than that of the smartphone magnetic sensor when passing through a door. The above results show that the smartphone magnetic sensors have large errors. Thus, in the future, we will explore how to calibrate the sensing error of smartphone magnetometer to further improve the performance of LMDD.

Further more, we evaluate the heterogeneity of magnetic sensors for different smartphones. Specifically, in our

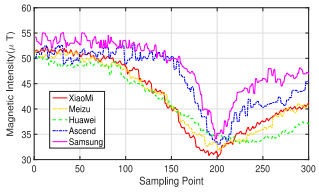

Fig. 27. Heterogeneity evaluation of smartphone magnetic sensors.

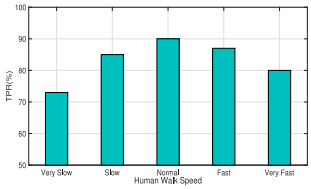

Fig. 28. The accuracy of LMDD in human walking speeds from $0.6m/s$ (very slow) to $3m/s$ (very fast).

experiment, we compare the magnetic sensors' readings of five smartphones, including Sumsang Galaxy S4, Huawei Ascend P7, Sony Xperia Z2, XiaoMi M2S, and Meizu MX. which are held by a user to walk through the same door. As shown in Fig. 27, the magnetic sensors' readings are different with the smartphones. The reason is that different phones have different vendors for their internal chips, which have influences on the sensor readings [2]. In addition, we observe that the variation ranges of magnetic intensity passing the same door are approximate, e.g., about $20\mu T$, though the absolute readings of different devices are different. Thus, we utilize the range Gaussian kernel to calculate the variation of magnetic intensities. The range feature is a relative variable and not affected by absolute readings seriously, thus greatly alleviating the influence of heterogeneous chips on LMDD. Finally, we evaluate the performance of LMDD with these five different smartphones in Fig. 23, which shows its detection accuracy is more than 80 percent on average. Hence, our schemes can effectively overcome the influence of device heterogeneity on the LMDD. In the future, we will explore the high-accuracy magneto-resistive magnetic sensor to calibrate the sensing errors of common smartphone magnetometers and use the crowd-sensing to weaken the influence of different internal chips on the LMDD accuracy.

Influence of Users' Behavior. First, we analyze the impact of walking speed on the performance. Since the average walking speed of indoor users is about $1.48 \sim 2.11$ m/s [33], the time difference is very small when a user passes through a door. For example, when a user walks slowly or fast through a door (about three meters' length), the time difference is less than 0.6 s. Thus, the walking speed of users through a door has slight influence on the time window size and the detection performance. Furthermore, we conduct extensive experiments to further verify this conclusion by comparing the performance of LMDD in different walking speeds of users. We change the speeds uniformly from 0.6 m/s (very slow) to 3 m/s (very fast). As shown in Fig. 28, the performances of LMDD in the slow (1.2 m/s), normal (1.8 m/s) and fast speeds (2.4 m/s) are similar, and all the TPRs are more than 85 percent. Moreover, if the speed is abnormal, e.g., very slow (about 0.6 m/s) or very fast (about 3 m/s) [33], though the TPRs are still above 72 percent, it is a little lower than that with normal speeds,

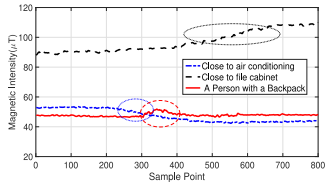

Fig. 29. The multiple factors in a complex indoor environment.

e.g., about 10 percent. It is because that the time window size and sampling frequency are set to constants for easy use in practice. Hence, the slower the speed, the shorter the walking distance in a time window, and the smaller the range of magnetic intensities, as illustrated in Fig. 9. (It is similar in the very fast speed.) As a result, when the speed is very slow or very fast, the range Gaussian kernel of magnetic intensities in a time windows becomes smaller and is less than the threshold, thus decreasing the detection accuracy slightly. In summary, the walking speed of users makes a negligible impact on the LMDD's performance.

Second, we discuss the influence of user's action and the door state on the LMDD's performance. When the door states (e.g., open/closed door or inside-swing/outside-swing door) or user's actions (e.g., open/close a door) change, the difference of magnetic field intensities between inside and outside of a room still keeps constant [23]. As the LMDD detects the door events based on the changes of magnetic field intensity when a user walks through the door, the door states and user's actions have a negligible impact on the performance of LMDD. In the future, we will explore how to diminish these influences so as to further improve the performance, e.g., using machine learning algorithms to learn user's behaviors based on their historical data [29], [34], [41].

Interference of Indoor Environments. In the complex indoor environment, various metallic objects may affect the magnetic intensity of magnetic sensors, thus decreasing the detection performance of LMDD. For example, when a smartphone is close to large metallic objects, such as electrical appliances, furniture, etc, the magnetic field will be changed. Thus, we make experiments to explore the negative influence of indoor environments on the detection performance of LMDD. As shown in the Fig. 29, when a smartphone is close to an air conditioning and a metallic file cabinet, the magnetic intensity is changed. Even when a person with a laptop backpack walks through a smartphone, the magnetic intensity will occur pulse change due to the interference from the inside laptop and metallic objects. According to the above observations, the complex indoor environments make a significant influence on the sensing data of magnetic sensor, which undermines the detection performance LMDD. Hence, in the future, we will explore to solve this problem by utilizing deep-learning scheme to build more accurate detection model based on a mass of door event detection data.

Crowdsensing of Massive Users. To alleviate the negative influences of sensor error and complex indoor environments, we can use the crowdsensing of massive users to improve the detection performance. In this section, we conduct a small-scale pilot experiment to explore the impact of crowdsensing on the performance of basic LMDD. We collect the sensing data from six volunteers when they pass through a door with Android-based smartphones. We compute the detection errors by making a majority voting decision based on the crowdsensing of these 6 users to evaluate the performance of LMDD. As shown in the Fig. 30, the

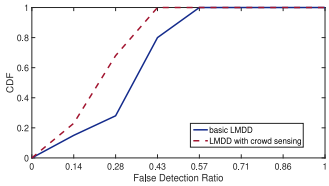

Fig. 30. Performance comparison between basic LMDD and crowdsensing-based LMDD.

worst false detection ratio of LMDD with crowdsensing is less than 45 percent but that of basic LMDD is more than 55 percent. Besides, the crowdsensing-based LMDD has the better performance with an increase of at least 33 percent in median false detection ratio over basic LMDD, which indicates the effectiveness of crowdsensing to improve the performance of LMDD. In the future, we will further explore how to use the crowdsensing [8], [32], [37] to improve the accuracy of door event detection.

Application of LMDD in Indoor Localization. As the ultimate goal of LMDD is to calibrate the indoor localization results in IPSes, we discuss how to apply LMDD to indoor localization as follows. First, we take a basic application of LMDD-based indoor localization as an example [31]. As shown in Fig. 1a, the localization error of a user in IPSes increases with his/her walking distance due to the accumulation error [25], [31]. When the user passes through a door, LMDD can accurately detect the door event based on the change of magnetic sensing data. After that, we can use the approximate localization of the user achieved from current IPSes (such as the dead-reckoning) to match the door position of the floor plan [35], which is then used to calibrate the inaccurate localization of the user. Moreover, in practice, the user's position may match the false door positions due to the large error of the approximate localization or short distances between doors. To address this problem, we can use the fine-grained features of magnetic intensity to identify each door, since different material, structure and/or size of doors make the fine-grained diversity of the magnetic sensing data [29]. Also, we can use other inertial sensors of smartphones to distinguish the adjacent doors. e.g., the Gyroscope sensing data can be used to identify the left-side/right-side doors of the corridor due to different turning directions [29], [41]. These researches are deferred to the future work, while this paper mainly focuses on the accurate door event detection.

7 Conclusion

Doors are important landmarks for indoor positioning systems. An accurate and light-weight door event detection approach is therefore highly desired. In this paper, we observe special change patterns of magnetic signals when carrying a smartphone to pass through a door. Based on this observation, we design a light-weight, magnetic-based infrastructure-free door event detection approach (named LMDD) running on common smartphones. A signal analysis algorithm combined with a feature correlation function is designed to capture door events and cancel environmental events. In order to further improve the robustness and accuracy of LMDD, an improved door event detection framework based on a majority-voting model to fuse multiple-dimensional sensing data from non-magnetic built-in sensors. Prototype experiments in various typical environments show that LMDD achieves sound door event detection accuracy. We believe that our proposed door event detection method would significantly benefit indoor positioning systems.

Acknowledgments

This research is supported by the National Key R&D Program of China under grant 2018YFB1004700, the NSF of China Projects No. 61872447, 61772546, 61625205, 61272429, and 61632010, and the NSF of Jiangsu for Distinguished Young Scientist BK20150030.

References

[1] H. Abdelnasser, R. Mohamed, A. Elgohary, M. F. Alzantot, H. Wang, S. Sen, R. R. Choudhury, and M. Youssef, "SemanticSLAM: Using environment landmarks for unsupervised indoor localization," *IEEE Trans. Mobile Comput.*, vol. 15, no. 7, pp. 1770–1782, Jul. 2016.

[2] S. Ali and S. Khusro, "Mobile phone sensing: A new application paradigm," *Indian J. Sci. Technol.*, vol. 9, no. 19, pp. 1–42, 2016.

[3] D. Anguelov, D. Koller, E. Parker, and S. Thrun, "Detecting and modeling doors with mobile robots," in *Proc. Int. Conf. Robot. Autom.*, 2004, pp. 3777–3784.

[4] M. Bahrepour, N. Meratnia, M. Poel, Z. Taghikhaki, and P. J. M. Havinga, "Distributed event detection in wireless sensor networks for disaster management," in *Proc. Int. Conf. Intell. Netw. Collaborative Syst.*, 2010, pp. 507–512.

[5] G. Bin, S. S. Victor, K. Y. Tay, R. Walter, and L. Shuo, "Incremental support vector learning for ordinal regression," *IEEE Trans. Neural Netw. Learn. Syst.*, vol. 26, no. 7, pp. 1403–1416, Jul. 2017.

[6] G. Bin, S. Xingming, and S. S. Victor, "Structural minimax probability machine," *IEEE Trans. Neural Netw. Learn. Syst.*, vol. 28, no. 7, pp. 1646–1656, Jul. 2017.

[7] C. Chen, S. Jiao, S. Zhang, W. Liu, L. Feng, and Y. Wang, "Triplmputor: Real-time imputing taxi trip purpose leveraging multi-sourced urban data," *IEEE Trans. Intell. Transp. Syst.*, vol. 19, no. 10, pp. 3292–3304, Oct. 2018.

[8] C. Chen, D. Zhang, X. Ma, B. Guo, L. Wang, Y. Wang, and E. Sha, "CrowdDeliver: Planning city-wide package delivery paths leveraging the crowd of taxis," *IEEE Trans. Intell. Transp. Syst.*, vol. 18, no. 6, pp. 1478–1496, Jun. 2017.

[9] C. Cheng and T. Yingli, "Door detection via signage context-based hierarchical compositional model," in *Proc. IEEE Comput. Soc. Conf. Comput. Vis. Pattern Recognit.*, 2010, pp. 1–6.

[10] J. Chung, M. Donahoe, C. Schmandt, I. J. Kim, P. Razavai, and M. Wiseman, "Indoor location sensing using geo-magnetism," in *Proc. Int. Conf. Mobile Syst. Appl. Services*, 2011, pp. 141–154.

[11] S. K. Divvala, D. Hoiem, J. H. Hays, and A. A. Efros, "An empirical study of context in object detection," in *Proc. IEEE Conf. Comput. Vis. Pattern Recognit.*, 2009, pp. 1271–1278.

[12] B. Gozick, K. P. Subbu, R. Dantu, and T. Maeshiro, "Magnetic maps for indoor navigation," *IEEE Trans. Instrum. Meas.*, vol. 60, no. 12, pp. 3883–3891, Dec. 2011.

[13] F. Gu, A. Kealy, K. Khoshelham, and J. Shang, "Efficient and accurate indoor localization using landmark graphs," *Int. Archives Photogrammetry Remote Sens. Spatial Inf. Sci.*, vol. XLI-B2, pp. 509–514, 2016.

[14] J. Haverinen and A. Kemppainen, "Global indoor self-localization based on the ambient magnetic field," *Robot. Auton. Syst.*, vol. 57, no. 10, pp. 1028–1035, 2009.

[15] J. Hensler, M. Blaich, and O. Bittel, "Real-time door detection based on adaboost learning algorithm," *Res. Edu. Robot.*, EUROBOT, vol. 82, pp. 61–73, 2009.

[16] T. W. Hnat, E. Griffiths, R. Dawson, and K. Whitehouse, "Doorjamb: Unobtrusive room-level tracking of people in homes using doorway sensors," in *Proc. ACM Conf. Embedded Netw. Sensor Syst.*, 2012, pp. 309–322.

[17] K. Kaji and N. Kawaguchi, "Gate-passing detection method using WiFi and accelerometer," in *Transactions on Engineering Technologies : Special Volume of the World Congress on Engineering 2013*. Berlin, Germany: Springer, 2014, pp. 439–453.

[18] P. Kim, B. Coltin, O. Alexandrov, and H. J. Kim, "Robust visual localization in changing lighting conditions," in *Proc. IEEE Int. Conf. Robot. Autom.*, 2017, pp. 5447–5452.

[19] R. Liu, C. Yuen, T. N. Do, Y. Jiang, X. Liu, and U. X. Tan, "Indoor positioning using similarity-based sequence and dead reckoning without training," in *Proc. IEEE Int. Workshop Signal Process. Advances Wireless Commun.*, 2017, pp. 1–5.
[20] A. Mesaros, T. Heittola, A. Eronen, and T. Virtanen, "Acoustic event detection in real-life recordings," in *Proc. Signal Process. Conf. Eur.*, 2010, pp. 1267–1271.
[21] R. D. Morey, R. Hoekstra, J. N. Rouder, M. D. Lee, and E. J. Wagenmakers, "The fallacy of placing confidence in confidence intervals," *Psychonomic Bulletin Rev.*, vol. 23, no. 1, pp. 103–123, 2016.
[22] C. Pal, A. Chakrabarti, and R. Ghosh, "A brief survey of recent edge-preserving smoothing algorithms on digital images," *Comput. Sci.*, arXiv: 1503.07297v1, 2015.
[23] V. Pasku, A. De Angelis, A. Moschitta, P. Carbone, J. O. Nilsson, S. Dwivedi, and P. Hndel,"A magnetic ranging-aided dead-reckoning positioning system for pedestrian applications," *IEEE Trans. Instrum. Meas.*, vol. 6, no. 5, pp. 953–963, May 2017.
[24] A. Rai, K. K. Chintalapudi, V. N. Padmanabhan, and R. Sen, "Zee: Zero-effort crowdsourcing for indoor localization," in *Proc. Annu. Int. Conf. Mobile Comput. Netw.*, 2012, pp. 293–304.
[25] W. Sakpere, M. A. Oshin, and N. B. W. Mlitwa, "A state-of-the-art survey of indoor positioning and navigation systems and technologies," *South African Comput. J.*, vol. 29, no. 3, 2017, Art. no. 145.
[26] R. W. Schafer, "What is a Savitzky-Golay filter [lecture notes]," *IEEE Signal Process. Mag.*, vol. 28, no. 4, pp. 111–117, Jul. 2011.
[27] L. Shangguan, Z. Yang, A. X. Liu, Z. Zhou, and Y. Liu, "STPP: Spatial-temporal phase profiling-based method for relative RFID tag localization," *IEEE/ACM Trans. Netw.*, vol. 25, no. 1, pp. 596–609, Feb. 2017.
[28] K. P. Subbu, B. Gozick, and R. Dantu, "LocateMe: Magnetic-fields-based indoor localization using smartphones," *Trans. Intell. Syst. Technol.*, vol. 4, no. 4, pp. 73:1–73:27, 2013.
[29] H. Suining and G. S. Kang, "Geomagnetism for smartphone-based indoor localization: Challenges, advances, and comparisons," *ACM Comput. Surveys*, vol. 50, no. 6, pp. 1–37, 2017.
[30] Y. Tian, X. Yang, and A. Arditi, "Computer vision-based door detection for accessibility of unfamiliar environments to blind persons," in *Proc. Int. Conf. Comput. Helping People Special Needs*, 2010, pp. 263–270.
[31] H. Wang, S. Sen, A. Elgohary, M. Farid, M. Youssef, and R. R. Choudhury, "No need to war-drive: Unsupervised indoor localization," in *Proc. Int. Conf. Mobile Syst. Appl. Services*, 2012, pp. 197–210.
[32] Y. Wang, Z. Cai, G. Yin, Y. Gao, X. Tong, and G. Wu, "An incentive mechanism with privacy protection in mobile crowdsourcing systems," *Comput. Netw.*, vol. 102, pp. 157–171, 2016.
[33] C. Willn, "Walking speed indoors and outdoors in healthy persons," in *Proc. Human Factors Ergonom. Soc. Annu. Meet.*, 2013, pp. 213–217.
[34] C. Wu, Z. Yang, and Y. Liu, "Smartphones based crowdsourcing for indoor localization," *IEEE Trans. Mobile Comput.*, vol. 14, no. 2, pp. 444–457, Feb. 2015.
[35] C. Wu, Z. Yang, and C. Xiao, "Automatic radio map adaptation for indoor localization using smartphones," *IEEE Trans. Mobile Comput.*, vol. 17, no. 3, pp. 517–528, Mar. 2018.
[36] Z. Wu, Q. Xu, J. Li, C. Fu, Q. Xuan, and Y. Xiang, "Passive indoor localization based on CSI and Naive Bayes classification," *IEEE Trans. Syst. Man Cybern. Syst.*, vol. 48, no. 9, pp. 1566–1577, Sep. 2018.
[37] C. Xiang, P. Yang, C. Tian, L. Zhang, H. Lin, F. Xiao, M. Zhang, and Y. Liu, "CARM: Crowd-sensing accurate outdoor RSS maps with error-prone smartphone measurements," *IEEE Trans. Mobile Comput.*, vol. 15, no. 11, pp. 2669–2681, Nov. 2016.
[38] F. Xiao, Z. Wang, N. Ye, R. Wang, and X. Y. Li, "One more tag enables fine-grained RFID localization and tracking," *IEEE/ACM Trans. Netw.*, vol. 26, no. 1, pp. 161–174, Feb. 2018.
[39] H. Xu, Z. Yang, Z. Zhou, L. Shangguan, K. Yi, and Y. Liu, "Enhancing WiFi-based localization with visual clues," in *Proc. ACM Int. Joint Conf. Pervasive Ubiquitous Comput.*, 2015, pp. 963–974.
[40] Z. Yang, C. Wu, and Y. Liu, "Locating in fingerprint space: Wireless indoor localization with little human intervention," in *Proc. Annu. Int. Conf. Mobile Comput. Netw.*, 2012, pp. 269–280.
[41] Z. Yang, C. Wu, Z. Zhou, X. Zhang, X. Wang, and Y. Liu, "Mobility increases localizability: A survey on wireless indoor localization using inertial sensors," *ACM Comput. Surveys*, vol. 47, no. 3, pp. 1–34, 2015.
[42] Z. Yilin, "Mobile phone location determination and its impact on intelligent transportation systems," *Trans. Intell. Transp. Syst.*, vol. 1, no. 1, pp. 55–64, 2000.
[43] Z. Yin, C. Wu, Z. Yang, and Y. Liu, "Peer-to-peer indoor navigation using smartphones," *IEEE J. Sel. Areas Commun.*, vol. 35, no. 5, pp. 1141–1153, May 2017.
[44] Y. Zhao, C. Qian, L. Gong, Z. Li, and Y. Liu, "LMDD: Light-weight magnetic-based door detection with your smartphone," in *Proc. 44th Int. Conf. Parallel Process.*, 2015, pp. 919–928.
[45] Y. Zheng, G. Shen, L. Li, C. Zhao, M. Li, and F. Zhao, "Travi-Navi: Self-deployable indoor navigation system," in *Proc. 20th Annu. Int. Conf. Mobile Comput. Netw.*, 2014, pp. 471–482.
[46] Z. Zhou, Z. Yang, C. Wu, L. Shangguan, and Y. Liu, "Omnidirectional coverage for device-free passive human detection," *IEEE Trans. Parallel Distrib. Syst.*, vol. 25, no. 7, pp. 1819–1829, Jul. 2014.
[47] H. Zhu, F. Xiao, L. Sun, R. Wang, and P. Yang, "R-TTWD: Robust device-free through-the-wall detection of moving human with WiFi," *IEEE J. Sel. Areas Commun.*, vol. 35, no. 5, pp. 1090–1103, May 2017.
[48] T. Zou, S. Lin, and S. Li, "Blind RSSD-based indoor localization with confidence calibration and energy control," *Sensors*, vol. 16, no. 6, 2016, Art. no. 788.

Liangyi Gong received the BE and PhD degrees from Harbin Engineering University, China, in 2010 and 2016, respectively. He is a postdoc researcher with the School of Software and BNRist, Tsinghua University, and an assistant professor with the School of Computer Science and Engineering, Tianjin University of Technology, China. His major research interests cover mobile/pervasive computing and network security.

Yiyang Zhao received the BSc degree from Tsinghua University, in 1998, the MSc degree from the Institute of Electrical Engineering, Chinese Academy of Sciences, in 2001, and the PhD degree from the Hong Kong University of Science and Technology, in 2010. He is a chief scientist of AI labs with the Simple Educational Corporation. He served as a postdoc researcher with the School of Software and TNLIST, Tsinghua University. His research interests include artificial intelligence and IoT.

Chaocan Xiang received the BS and PhD degrees in computer science and engineering from the Institute of Communication Engineering, PLA University of Science and Technology, China, in 2009 and 2014, respectively. He is currently an assistant professor with Chongqing University and the Army Logistics University of PLA, China. His current research interests include mobile/pervasive computing, crowd-sensing networks, and IoT.

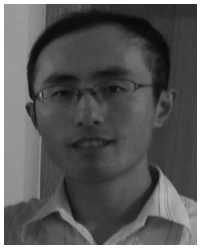

Zhenhua Li received the BSc and MSc degrees in computer science and technology from Nanjing University, in 2005 and 2008, respectively, and the PhD degree in computer science and technology from Peking University, in 2013. He is an assistant professor with the School of Software and BNRist, Tsinghua University. His research areas mainly consist of cloud computing/storage, content distribution, and mobile Internet. He is a member of the IEEE.

Chen Qian received the BSc degree from Nanjing University, in 2006, the MPhil degree from the Hong Kong University of Science and Technology, in 2008, and the PhD degree from the University of Texas at Austin, in 2013. He is an assistant professor with the Department of Computer Engineering, University of California, Santa Cruz. He was an assistant professor with the Department of Computer Science, University of Kentucky, in 2013-2016. His research interests include computer networking and IoT. He is a member of the IEEE.

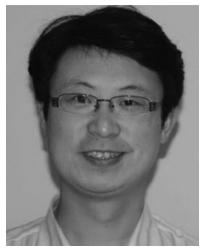

Panlong Yang received the BS, MS, and PhD degrees in communication and information system from the Nanjing Institute of Communication Engineering, China, in 1999, 2002, and 2005, respectively. He is now a professor with the School of Computer Science and Technology, University of Science and Technology of China. His research interests include mobile/pervasive computing and IoT. He is a member of the IEEE.